NANO LETTERS

pubs.acs.org/NanoLett

DNA-Mediated Control of Metal Nanoparticle Shape: One-Pot Synthesis and Cellular Uptake of Highly Stable and Functional Gold Nanoflowers

Zidong Wang,[†,||] Jieqian Zhang,[‡] Jonathan M. Ekman,[||] Paul J. A. Kenis,[§,||] and Yi Lu*[,†,‡,||]

[†]Department of Materials Science and Engineering, [‡]Department of Chemistry, [§]Department of Chemical & Biomolecular Engineering, and [||]Beckman Institute for Advanced Science and Technology, University of Illinois at Urbana−Champaign, Urbana, Illinois 61801

ABSTRACT The effects of different DNA molecules of the same length on the morphology of gold nanoparticles during synthesis are investigated. While spherical nanoparticles (AuNS) are observed in the presence of 30-mer poly T, like that in the absence of DNA, 30-mer poly A or poly C induces formation of the flower-shaped gold nanoparticle (AuNF). Detailed mechanistic studies indicate that the difference in DNA affinity to the AuNP plays a major role in the different morphology control processes. The DNA adsorbed on the AuNS surface could act as template to mediate the formation of flower-like gold nanoparticles. The formation of the AuNF can result from either selective deposition of the reduced gold metal on AuNS templated by surface bound DNA or uneven growth of the AuNS due to the binding of DNA to the surface. Furthermore, DNA functionalization with high stability was realized in situ during the one-step synthesis while retaining their biorecognition ability, allowing programmable assembly of new nanostructures. We have also shown that the DNA-functionalized nanoflowers can be readily uptaken by cells and visualized under dark-field microscopy.

KEYWORDS DNA, shape control, nanoparticle synthesis, gold nanoflowers, cellular uptake

Over the past decade, growing interest and research investigations have been focused on metal nanoparticles due to their unique physicochemical properties and potential applications in selective catalysis, sensitive sensing, and enhanced imaging.[1−9] The properties of a metal nanoparticle are greatly affected by its size, shape, and crystal structure, and therefore it is possible to tune the properties of the particle by controlling its growth process. Toward shape-controlled nanoparticle synthesis, molecular capping agents such as organic surfactants and polymers have been used to direct nanocyrstal growth in a face selective fashion.[8,9] Despite tremendous progress, the mechanism of the shape control is not well understood, in part due to the difficulty in defining structures and conformations of these surfactants and polymers in solution and in systematic variation of functional groups.

DNA is a well-known biopolymer with more defined structure and conformation in solution and unique programmable nature to tune its functional properties.[10−13] Because of these advantages, DNA has been used as template to position nanoparticles through DNA metallization,[14,15] or nanoparticle attachment,[16−21] or to control the sizes and the photoluminescent property of quantum dots.[22−28] However, in contrast to proteins or peptides,[29−32] DNA has been much less explored to control the shape or morphology of metal nanoparticles, and therefore, the promise of this field remains to be fully realized. Such an investigation may result in new nanoparticles with new shapes and offer deeper insights into mechanisms of shape control. Here we demonstrate a new method to use DNA for modulating the shape and thus the optical properties of gold nanoparticles. Systematic variations of the DNA sequences offer mechanistic insights into the morphology control. We also show that DNA in such nanoparticles maintains its bioactivity, allowing programmable assembly of new nanostructures. In addition, the cell uptake ability and light scattering property of the flower-shaped nanoparticles are also demonstrated.

Single-strand DNA (ssDNA) has been found to adsorb on citrated coated gold nanospheres (AuNSs) in a sequence-dependent manner.[33] Deoxynucleosides dA, dC, and dG have shown much higher binding affinity to gold surfaces than deoxynucleoside dT.[34] However, the effect of different DNA sequences on gold nanoparticle morphology during crystal growth has not been investigated. To investigate this effect, we chose three types of 30-mer DNAs consisting of poly A, poly C, and poly T (designated as A30, C30, and T30) and 20 nm citrate-coated AuNSs as the seeds for nanoparticle growth. Hydroxylamine (NH_2OH) has been shown to perform the reduction of hydrogen tetrachloroaurate(III) ($HAuCl_4$) catalyzed by the gold surface[35] and thus is chosen as the reducing agent in this work. In a typical synthesis,

* To whom correspondence should be addresses: e-mail, yi-lu@illinois.edu; phone, 217-333-2619; fax, 217-244-3186.

Received for review: 02/24/2010
Published on Web: 04/20/2010

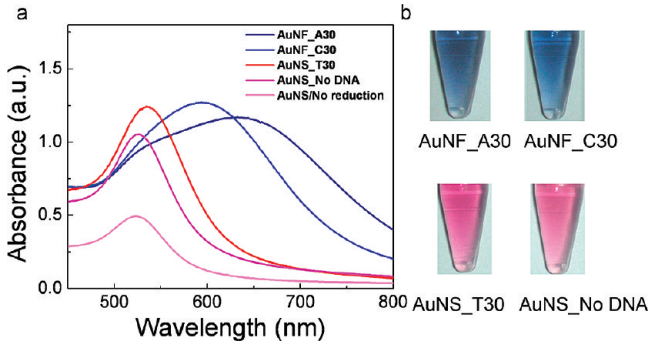

FIGURE 1. (a) UV−vis spectra of the gold nanoparticle solutions prepared with the addition of A30 (dark blue line), C30 (blue line), T30 (red line), or without adding DNA (pink line) or before reduction (light pink line). (b) Images of corresponding gold nanoparticles in a centrifuge tube with the addition of different DNAs or without DNA.

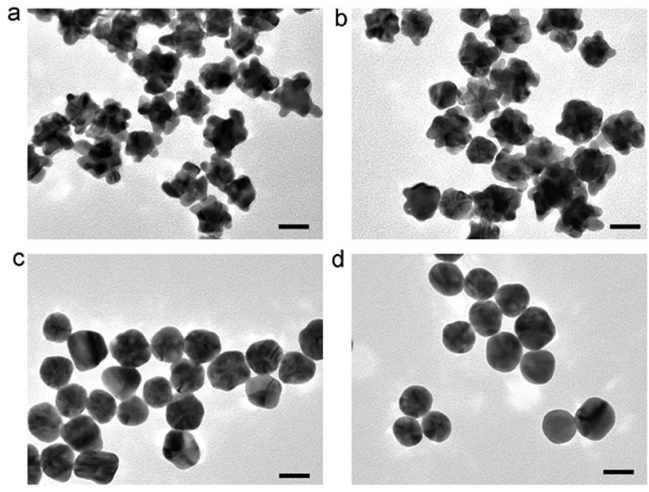

FIGURE 2. TEM images of gold nanoparticles prepared with (a) A30, (b) C30, and (c) T30 (d) in the absence of DNA. The scale bar indicates 20 nm.

AuNSs (0.5 nM) were first incubated with DNA (1 μM) for 15 min to allow adsorption of DNA onto AuNS followed by addition of 20 mM NH_2OH. $HAuCl_4$ (167 μM) was then introduced, and the mixture was rigorously vortexed to facilitate the reduction. Surprisingly, nanoparticle solutions synthesized in the presence of A30 or C30 were blue colored, while the nanoparticle solution synthesized with T30 was red colored (Figure 1). The resultant solutions were stable for days without showing any nanoparticle aggregation or color change.

To find out the morphology of the nanoparticles prepared with different DNA sequences, transmission electron microscopy (TEM) was employed to investigate each of the resulting nanoparticle solutions. Interestingly, those particles synthesized with A30 or C30 are flower shaped (designated as AuNF_A30 and AuNF_C30) (Figure 2, panels a and b), while particles synthesized with T30 are spherical (AuNP_T30) (Figure 2c). The flower-shaped gold nanoparticles have a broad surface plasmon absorbance that peaks at 600 nm (for AuNF_C30) or 630 nm (for AuNF_A30) (Figure 1a), which are consistent with the absorbance of gold nanoflowers (AuNFs) prepared by other reported methods.[36] Poly G30 was not tested here due to synthetic difficulties caused by the formation of a guanine tetraplex structure.[37] Instead, a shorter DNA consisting of 10-mer poly G was tested, and the resulting nanoparticles were nearly spherical (Figure S1 in Supporting Information). In contrast, only spherical nanoparticles were formed in the absence of DNA (Figure 2d) or in the presence of salt only (Figure S2 in Supporting Information). No metal nanoparticles were formed upon mixing DNA, NH_2OH, and $HAuCl_4$ together, without the addition of AuNS as seeds. These results show that it is the DNA that mediates the morphology of the gold nanoparticles and the nanoparticle shape is sequence dependent.

To understand this DNA-sequence-dependent nanoparticle formation, we first investigated the adsorption step of ssDNA on AuNS. Unmodified ssDNA is able to adsorb onto AuNS and enhance the electrostatic repulsion between AuNSs and prevent them from salt-induced aggregation.[38] We incubated same amounts of different DNA sequences with AuNS separately, and then challenged the AuNS solution with 0.1 M NaCl. As shown in Figure S3 (Supporting Information), aggregation of AuNS happened immediately when the T30 DNA sequence was used for incubation with the AuNS, while AuNS incubated with A30 or C30 sequences remained stable. Since the stability of the AuNS at the same salt concentration is determined by the number of DNA adsorbed on its surface,[39] we can conclude that much fewer T30 were adsorbed onto a AuNS surface compared to A30 or C30, which is consistent with the lower binding affinity of T30 toward the gold nanoparticle surface. This result, therefore, explains the differences in shaping the gold nanoparticle by the T30 sequence in comparison with A30 or C30.

To obtain deeper insight into the mechanism of shape control process of the flower-shaped nanoparticle directed by DNA, we added varying amounts of $HAuCl_4$ to A30, which was incubated with AuNS and 20 mM NH_2OH to initiate the reduction. Since NH_2OH is in large excess, the $HAuCl_4$ should be completely reduced to gold metal in the presence of AuNS seeds.[35] As shown in Figure S4 (Supporting Information), with the addition of increasing amounts of $HAuCl_4$, the resultant nanoparticle evolved from sphere shape to a budding sphere and then into the flower-like shape. Upon further increase of the $HAuCl_4$ amount, the flower-shaped nanoparticle would grow even bigger.

In order to investigate how the nanoparticle morphology could be affected by the number of DNA adsorbed on AuNS, varying amounts of A30 were incubated with AuNS and followed by reduction of equal amounts of $HAuCl_4$. Figure S5 (Supporting Information) shows that the nanoparticle shape changed from spherical to flower-like

DOI: 10.1021/nl100675p | *Nano Lett.* **2010,** *10,* 1886–1891

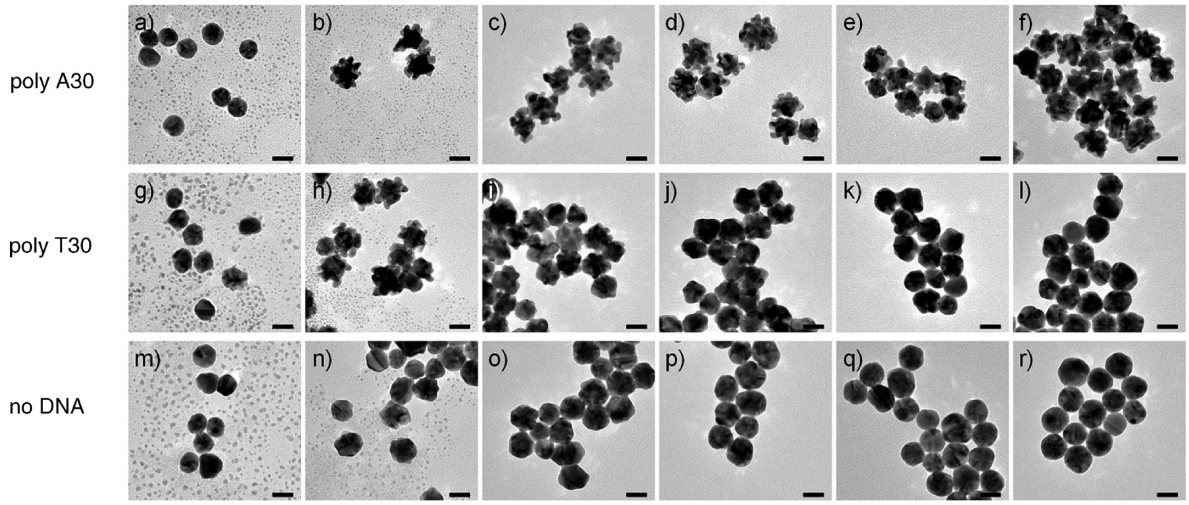

FIGURE 3. TEM images of the nanoparticle intermediates prepared by stopping the nanoparticle growth with mercaptopropionic acid (1.5 mM) after 0.5 s (a, g, m) 2 s (b, h, n), 5 s (c, i, o), 30 s (d, j, p), 5 min, (e, k, q) and 15 min (f, l, r) of the reaction. The images in the top row (a−f) represent the intermediates synthesized in the presence of poly A30. The images in the second row (g−l) represent the intermediates synthesized in the presence of poly T30. The images in the last row (m−r) represent the intermediates synthesized in the absence of DNA. Before initiation of the reduction reaction, 100 μL of 0.5 nM AuNS solution was incubated with 1 μM DNA. The scale bar indicates 20 nm.

with increasing numbers of DNA adsorbed on AuNS, while the size of the gold nanoparticle remained the same. From the above observations, we conclude that DNA of chain-like structure was able to direct the deposition of the reduced gold metal on the AuNS and guide the nanoparticle growth from a spherical into a flower-like shape. This hypothesis was further supported by the control experiments which showed that when the single deoxynucleotide, adenosine monophosphate (AMP) was incubated with AuNS instead of a DNA chain, the nanoparticles obtained were nearly spherical, while a random 30-mer DNA sequence of mixed A, T, G, or C caused the formation of flower-shaped nanoparticles (Figure S6 in Supporting Information).

To further probe this DNA-mediated AuNF growing process, we monitored the absorbance of AuNF growth solution using UV−visible spectrometer. As shown in Figure S7 (Supporting Information), after initiation of the reaction for 3 s, the intensity of the nanoparticle absorbance increased significantly and the peak of the AuNSs at 520 nm broadened and red-shifted. With growth of the AuNS, a new absorbance peak at 630 nm from the resultant AuNFs appeared and the reaction completed in about 15 min. This time-dependent AuNF growth process was further studied using TEM by stopping the reaction at the early stages of NP growth with excess mercaptopropionic acid (MPA). MPA has been shown to quench the NP growth effectively by forming less reactive Au(I)−MPA complex with gold ion.[40] As shown in Figure 3, both the 20 nm AuNSs and 1− 3 nm small nanoparticles (SNPs) could be observed after initiation of the reaction at 0.5 s. Further control experiment showed that formation of the SNPs could be due to the conversion of Au(I)−MPA complex into metal particles on the TEM grid upon electron-beam irradiation during TEM imaging (Figure S8 in Supporting Information). Flower-like nanoparticle intermediates were observed after 2 s of reaction in both A30- and T30-mediated syntheses. Interestingly, the flower-like intermediates prepared with T30 grew further into nanospheres within 30 s while the intermediates prepared with A30 maintained their flower-like structure and stable AuNFs were produced. In the absence of DNA, the AuNSs grew into bigger nanospheres and no flower-like intermediate was observed. These results suggest that DNA adsorbed on the AuNS surface could act as template to mediate the formation of a flower-like gold nanoparticle. The formation of the AuNF can result from either selective deposition of the reduced gold metal on AuNS templated by surface-bound DNA or uneven growth of the AuNS due to the binding of DNA to the surface. As depicted in Figure S9 (Supporting Information), due to the strong binding affinity of poly A or poly C to AuNS, a number of A30 or C30 bind tightly to AuNS and induce the inhomogeneous growth of AuNS, producing the flower-like nanoparticles. In contrast, fewer poly T bind weakly and loosely to AuNS, and it produce the flower-like intermediates only at the very initial stage but are not able to stabilize the flower-like structures and the spherical particles are eventually formed. A more detailed study on the mechanism is under way.

Biofunctionalization of the nanomaterials is crucial because it endows the nanomaterials with target recognition ability and enables their controlled assembly.[41] This functionalization step is not trivial and usually carried out separately as it requires delicate chemical modifications on the nanoparticles or the biomolecules to allow conjugation. Since our synthesized AuNFs are very stable in aqueous solution even in the presence of 0.3 M salt, we

DOI: 10.1021/nl100675p | *Nano Lett.* **2010,** *10,* 1886–1891

hypothesize that DNA can be attached to the nanoparticles during their synthesis and act as stabilizing ligands. To determine the number of oligonucleotides on each AuNF, we used a fluorophore (FAM) labeled poly A30 for AuNF synthesis. The average number of attached oligonucleotides on each AuNF was estimated to be ~359 by measuring the quantity of DNA in the supernatant after removing the AuNFs with centrifugation and comparing it with the initial DNA quantity used for AuNF synthesis. To probe the stability of the DNA attached to AuNFs, we treated the AuNFs solution with mercaptoethanol (ME) to a final concentration of 14 mM overnight and then the displaced oligonucleotides were quantified by fitting the fluorescence intensity of the supernatant to a standard linear calibration curve (see Supporting Information for a detailed procedure). We found out only ~110 strands were replaced by MCH, and the majority (~240 strands) was still bound to AuNF after the treatment. Thiol−gold chemistry is the most used method to conjugate DNA to gold surface. Under the same ME (14 mM) treatment, however, all of the thiolated DNA were displaced by ME from the gold surface.[42] Therefore, our in situ synthesis and controlled reduction method can realize DNA functionalization on gold surface with high stability but no requirement for chemical modifications on the DNA.

Considering the remarkably high binding affinity of DNA to the AuNFs (higher than thiol−gold binding), we hypothesized that the DNA in situ attached to AuNFs during reduction could be partially buried in the AuNFs. To test this hypothesis and also the functionality of the DNA on the AuNFs, we carried out experiments to test the melting point of the DNA in situ attached on the AuNFs. AuNFs were first treated with thiolated PEG molecule overnight to displace the weakly bound DNA and eliminate the nonspecific binding of DNA on AuNF surface.[43] Purified AuNF_A30 was hybridized with fluorophore (FAM) labeled poly T30 (FAM−T30) in a buffer solution containing 10 mM HEPES buffer (pH 7.1) and 50 mM NaCl. A fluorimetor coupled with a temperature controller was used to obtain the melting curve of the DNA hybridization on AuNFs. Since gold nanoparticle can effectively quench the fluorescence from its surrounding fluorophores, the release of the fluorophore labeled DNA from AuNFs due to DNA melting will result in a fluorescence increase of the nanoparticle solution. As a comparison, free A30 labeled with an organic quencher (Blank Hole Quencher-1) was hybridized with FAM−T30 in the same buffer under identical conditions and its melting curve was collected as well. As shown in Figure S10 (Supporting Information), the melting temperature of the DNA in situ attached to AuNFs (around 42 °C) was significantly lower than that of the free DNA (around 50 °C). This result indicated that a small segment of DNA might be buried in the AuNFs during the nanoparticle growth, while the majority of DNA exposed outside was still functional for DNA hybridization.

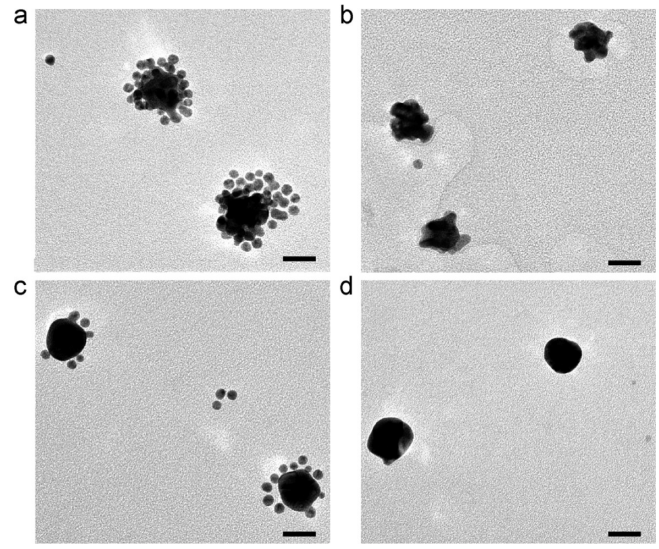

FIGURE 4. TEM images of the nanoassemblies: (a) AuNF_A30 with AuNS5nm_S_T30; (b) AuNF_A30 with noncomplementary AuNS5nm_S_A30; (c) AuNS_T30 with AuNS5nm_S_A30; (d) AuNS_T30 with noncomplementary AuNS5nm_S_T30. The scale bar indicates 20 nm.

To explore the application of these AuNFs in biodirected nanoassembly, AuNF_A30 particles were first treated with thiolated PEG molecules and purified. These nanoparticles were then incubated with 5 nm AuNS modified with thiolated cDNA T30 (AuNS5 nm_S_T30) in a ratio of 1:100 in buffer solution overnight. TEM was then employed to assess the assembly of the nanoparticles. As shown in Figure 4, AuNF_A30 was surrounded by a number of AuNS5nm_S_T30, forming the satellite structure. As a comparison, when 5 nm of AuNS functionalized with noncomplementary DNA A30 (AuNS5nm_S_A30) was used to incubate with AuNF_A30, no assembly was observed (Figure 4b). Additional large area TEM images containing multiple satellite assembled nanostructures are shown in Figure S11 (Supporting Information). These results further confirmed that the DNA molecules not only were densely functionalized to AuNFs in a large number but also retained their molecule recognition properties. Interestingly, when AuNS_T30 were incubated with AuNS5nm_S_A30 under similar conditions, only a few 5 nm particles were assembled on AuNS_T30, while little assembly was observed with noncomplementary AuNS5nm_S_T30 (Figure 4c,d). This observation indicates that fewer numbers of T30 were attached during synthesis, consistent with the fact that fewer T30 were adsorbed on AuNS compared to A30 or C30.

We further explored the potential usage of the DNA-functionalized AuNFs as imaging agents and nanocarriers in cellular environment. The light scattering property of the AuNFs was first investigated using a dark-field microscopy coupled to a CCD digital camera. The digital camera was white-balanced so that the observed colors represented the

DOI: 10.1021/nl100675p | *Nano Lett.* **2010,** *10,* 1886–1891

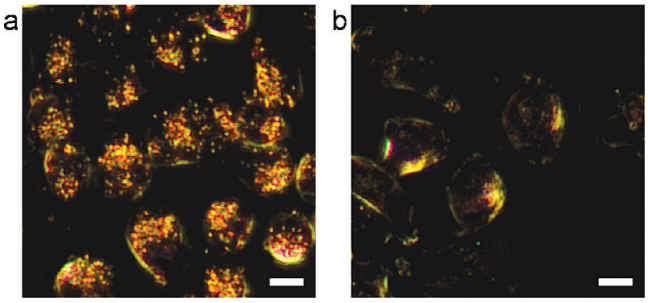

FIGURE 5. Dark field image of the CHO cells (a) treated with AuNF particles and (b) without nanoparticle treatment. The scale bar indicates 10 μm.

true color of the scattered light. The AuNFs showed bright orange color in the dark field image (Figure S12 in Supporting Information). To investigate the cell uptake of the AuNFs, 0.5 nM of AuNF particles synthesized with fluorophore (FAM) labeled A30 were incubated with CHO (Chinese hamster ovary) cells for 18 h and then excess AuNFs were removed by washing the cells with PBS buffer. Dark-field light-scattering images were taken to visualize the AuNFs uptaken by the cells.[44] As shown in Figure 5a, the orange dots representing the AuNFs were observed in the intracellular region of the cells while the untreated control cells appeared dim yellow to green color due to the intrinsic cellular scattering (Figure 5b). This nanoparticle cellular uptake was further confirmed by the 3D reconstructed confocal microscope images of the AuNF-treated cells, showing that the AuNFs were distributed inside the cells (see Figure S13 in Supporting Information). We conclude that AuNFs entered into cells during the incubation. This cellular uptake ability of the AuNF might be due to the high DNA loading on the AuNF surface[45] as well as the shape effect.[46] The cellular uptake ability and light scattering property make the AuNFs promising nanocarriers for drug or gene delivery and contrast agents for intracellular imaging.

In summary, we have demonstrated for the first time that DNA can be used to tune gold nanoparticle morphology in a sequence-dependent manner, suggesting that biomolecules can play a significant role in shaping nanoparticles. The mechanism of sequence-dependent shape control from spherical to flower-like nanoparticle is also elucidated. Furthermore, DNA functionalization with high stability was realized in situ during the one-step synthesis while retaining their biorecognition ability. We have also shown that the DNA-functionalized nanoflowers can be readily uptaken by cells and visualized under dark-field microscopy. These particles could find wide applications in fields such as bioinspired nanoassembly, biosensing, and biomedicine.

Acknowledgment. We thank Professor Catherine Murphy for advice and helpful discussions. This work has been supported by the National Science Foundation Center for Nanoscale Chemical-Electrical-Mechanical Manufacturing Systems (Nano-CEMMS) under NSF Award #0749028 (CMMI). Transmission emission microscopy was carried out at the Center for Microanalysis of Materials, University of Illinois, which is partially supported by the U.S. Department of Energy under Grant DEFG02-91-ER45439.

Supporting Information Available. Experimental details and additional figures. This material is available free of charge via the Internet at http://pubs.acs.org.

REFERENCES AND NOTES

(1) Murray, C. B.; Sun, S. H.; Doyle, H.; Betley, T. *MRS Bull.* **2001**, *26*, 985–991.
(2) Jin, R. C.; Cao, Y. W.; Mirkin, C. A.; Kelly, K. L.; Schatz, G. C.; Zheng, J. G. *Science* **2001**, *294*, 1901–1903.
(3) Jana, N. R.; Gearheart, L.; Murphy, C. J. *J. Phys. Chem. B* **2001**, *105*, 4065–4067.
(4) Sun, Y. G.; Xia, Y. N. *Science* **2002**, *298*, 2176–2179.
(5) Daniel, M. C.; Astruc, D. *Chem. Rev.* **2004**, *104*, 293–346.
(6) Sonnichsen, C.; Reinhard, B. M.; Liphardt, J.; Alivisatos, A. P. *Nat. Biotechnol.* **2005**, *23*, 741–745.
(7) Huang, X. H.; El-Sayed, I. H.; Qian, W.; El-Sayed, M. A. *J. Am. Chem. Soc.* **2006**, *128*, 2115–2120.
(8) Tao, A. R.; Habas, S.; Yang, P. D. *Small* **2008**, *4*, 310–325.
(9) Xia, Y.; Xiong, Y.; Lim, B.; Skrabalak, S. E. *Angew. Chem., Int. Ed.* **2009**, *48*, 60–103.
(10) Seeman, N. C. *Nature* **2003**, *421*, 427–431.
(11) Rothemund, P. W. K. *Nature* **2006**, *440*, 297–302.
(12) Lu, Y.; Liu, J. *Acc. Chem. Res.* **2007**, *40*, 315–323.
(13) Wang, Z.; Lu, Y. *J. Mater. Chem* **2009**, *19*, 1788–1798.
(14) Braun, E.; Eichen, Y.; Sivan, U.; Ben-Yoseph, G. *Nature* **1998**, *391*, 775–778.
(15) Gu, Q.; Cheng, C. D.; Gonela, R.; Suryanarayanan, S.; Anabathula, S.; Dai, K.; Haynie, D. T. *Nanotechnology* **2006**, *17*, R14–R25.
(16) Alivisatos, A. P.; Johnsson, K. P.; Peng, X.; Wilson, T. E.; Loweth, C. J.; Bruchez Jr, M. P.; Schultz, P. G. *Nature* **1996**, *382*, 609–611.
(17) Mirkin, C. A.; Letsinger, R. L.; Mucic, R. C.; Storhoff, J. J. *Nature* **1996**, *382*, 607–609.
(18) Warner, M. G.; Hutchison, J. E. *Nat. Mater.* **2003**, *2*, 272–277.
(19) Le, J. D.; Pinto, Y.; Seeman, N. C.; Musier-Forsyth, K.; Taton, T. A.; Kiehl, R. A. *Nano Lett.* **2004**, *4*, 2343–2347.
(20) Zhang, J.; Liu, Y.; Ke, Y.; Yan, H. *Nano Lett.* **2006**, *6*, 248–251.
(21) Lee, J. H.; Wernette, D. P.; Yigit, M. V.; Liu, J.; Wang, Z.; Lu, Y. *Angew. Chem., Int. Ed.* **2007**, *46*, 9006.
(22) Bigham, S. R.; Coffer, J. L. *J. Phys. Chem.* **1992**, *96*, 10581–10584.
(23) Ma, N.; Dooley, C. J.; Kelley, S. O. *J. Am. Chem. Soc.* **2006**, *128*, 12598–12599.
(24) Kumar, A.; Jakhmola, A. *Langmuir* **2007**, *23*, 2915–2918.
(25) Ma, N.; Yang, J.; Stewart, K. M.; Kelley, S. O. *Langmuir* **2007**, *23*, 12783–12787.
(26) Berti, L.; Burley, G. A. *Nat. Nanotechnol.* **2008**, *3*, 81–87.
(27) Wang, Q. B.; Liu, Y.; Ke, Y. G.; Yan, H. *Angew. Chem., Int. Ed.* **2008**, *47*, 316–319.
(28) Ma, N.; Sargent, E. H.; Kelley, S. O. *Nat. Nanotechnol.* **2009**, *4*, 121–125.
(29) Brown, S.; Sarikaya, M.; Johnson, E. *J. Mol. Biol.* **2000**, *299*, 725–735.
(30) Naik, R. R.; Stringer, S. J.; Agarwal, G.; Jones, S. E.; Stone, M. O. *Nat. Mater.* **2002**, *1*, 169–172.
(31) Banerjee, I. A.; Yu, L. T.; Matsui, H. *Proc. Natl. Acad. Sci. U.S.A.* **2003**, *100*, 14678–14682.
(32) Dickerson, M. B.; Sandhage, K. H.; Naik, R. R. *Chem. Rev.* **2008**, *108*, 4935–4978.
(33) Storhofff, J. J.; Elghanian, R.; Mirkin, C. A.; Letsinger, R. L. *Langmuir* **2002**, *18*, 6666–6670.
(34) Ostblom, M.; Liedberg, B.; Demers, L. M.; Mirkin, C. A. *J. Phys. Chem. B* **2005**, *109*, 15150–15160.
(35) Brown, K. R.; Natan, M. J. *Langmuir* **1998**, *14*, 726–728.

DOI: 10.1021/nl100675p | *Nano Lett.* **2010,** *10,* 1886–1891

(36) Bakr, O. M.; Wunsch, B. H.; Stellacci, F. *Chem. Mater.* **2006**, *18*, 3297–3301.
(37) Poon, K.; Macgregor, R. B. *Biopolymers* **1998**, *45*, 427–434.
(38) Li, H. X.; Rothberg, L. J. *J. Am. Chem. Soc.* **2004**, *126*, 10958–10961.
(39) Li, H. X.; Rothberg, L. *Proc. Natl. Acad. Sci. U.S.A.* **2004**, *101*, 14036–14039.
(40) Zhao, L.; Ji, X.; Sun, X.; Li, J.; Yang, W.; Peng, X. *J. Phys. Chem. C* **2009**, *113*, 16645–16651.
(41) Katz, E.; Willner, I. *Angew. Chem., Int. Ed.* **2004**, *43*, 6042–6108.
(42) Demers, L. M.; Mirkin, C. A.; Mucic, R. C.; Reynolds, R. A.; Letsinger, R. L.; Elghanian, R.; Viswanadham, G. *Anal. Chem.* **2000**, *72*, 5535–5541.
(43) Kannan, B.; Kulkarni, R. P.; Majumdar, A. *Nano Lett.* **2004**, *4*, 1521–1524.
(44) Wax, A.; Sokolov, K. *Laser Photonics Rev.* **2009**, *3*, 146–158.
(45) Giljohann, D. A.; Seferos, D. S.; Patel, P. C.; Millstone, J. E.; Rosi, N. L.; Mirkin, C. A. *Nano Lett.* **2007**, *7*, 3818–3821.
(46) Chithrani, B. D.; Ghazani, A. A.; Chan, W. C. W. *Nano Lett.* **2006**, *6*, 662–668.

DOI: 10.1021/nl100675p | *Nano Lett.* **2010,** *10,* 1886–-1891